Polymer Chemistry

PAPER

View Article Online
View Journal | View Issue



Cite this: *Polym. Chem.*, 2017, **8**, 272

# Stimulus-responsive non-ionic diblock copolymers: protonation of a tertiary amine end-group induces vesicle-to-worm or vesicle-to-sphere transitions†

Nicholas J. W. Penfold,[a] Joseph R. Lovett,[a] Pierre Verstraete,[b] Johan Smets[b] and Steven P. Armes*[a]

Received 21st June 2016,
Accepted 20th July 2016

DOI: 10.1039/c6py01076h

www.rsc.org/polymers

A well-defined poly(glycerol monomethacrylate) (PGMA) macromolecular chain transfer agent (macro-CTA) with a mean degree of polymerisation (DP) of 43 was prepared by reversible addition–fragmentation chain transfer (RAFT) polymerisation using a morpholine-functionalised trithiocarbonate-based chain transfer agent (MPETTC). Chain extension of this macro-CTA by RAFT aqueous dispersion polymerisation of 2-hydroxypropyl methacrylate (HPMA) at pH 7.0–7.5 produced a series of four MPETTC-PGMA$_{43}$-PHPMA$_y$ vesicles (where $y$ = 190, 200, 220 or 230). Protonation of the morpholine end-group increases the hydrophilic character of the PGMA stabiliser block, which leads to a reduction in the packing parameter for the diblock copolymer chains. However, such pH-responsive behaviour critically depends on the value of $y$. For $y$ = 190 or 200, lowering the solution pH to pH 3 induces a vesicle-to-worm transition at 20 °C according to dynamic light scattering, aqueous electrophoresis, transmission electron microscopy and turbidimetry studies. This order–order transition is suppressed in the presence of added electrolyte, which screens the cationic end-groups. In addition, no change in copolymer morphology was observed on lowering the solution temperature at neutral pH, regardless of the $y$ value. The diblock copolymer nano-objects obtained at pH 3 were also cooled to 4 °C to examine their dual stimulus-responsive behaviour to both pH and temperature triggers. In all four cases, a change in morphology from either worms or vesicles to afford spheres (or spheres plus relatively short worms) was observed. Temperature-dependent oscillatory rheology experiments performed on cationic worms at pH 3 indicated a worm-to-sphere transition on cooling from 20 °C to 4 °C, which leads to reversible degelation. In summary, spheres, worms or vesicles can be obtained for MPETTC-PGMA-PHPMA diblock copolymers on first lowering the solution pH to pH 3, followed by cooling from 20 °C to 4 °C.

## Introduction

The self-assembly of AB diblock copolymers to afford nanoparticles has been of considerable interest to many research groups over the last fifty years. Various copolymer morphologies have been reported in dilute solution,[1–9] with the most common being spheres, worms (often termed cylinders or rods) and vesicles (also known as polymersomes). Of particular interest are block copolymer vesicles, which have found applications as nano-reactors,[10,11] Pickering emulsifiers[12] and drug delivery vehicles.[13,14] In particular, stimulus-responsive vesicles have been designed to undergo morphological transformations on exposure to external stimuli such as temperature,[15] solution pH,[16,17] light irradiation[18,19] and addition of salt.[20] In some cases such vesicles can undergo one or more order–order transitions; for example, so-called 'schizophrenic' vesicles, can respond to external stimuli such as pH[21] or both pH and temperature.[22,23]

Block copolymer self-assembly has traditionally involved post-polymerisation processing, which is invariably conducted at low copolymer concentration (typically at less than 1% w/w solids). This is a potentially decisive disadvantage for many commercial applications. The development of reversible addition–fragmentation chain transfer (RAFT) polymerisation[24] has enabled the facile preparation of many functional

[a]*Department of Chemistry, University of Sheffield, Brook Hill, Sheffield, South Yorkshire, S3 7HF, UK. E-mail: s.p.armes@sheffield.ac.uk*
[b]*Procter & Gamble, Eurocor NV/SA, Temselaan 100, 1853 Strombeek-Bever, Belgium*

†Electronic supplementary information (ESI) available: Digital photographs of vesicle dispersion (pH 7) and worm dispersions (pH 3); additional TEM images of vesicle/worm mixed phases; temperature-dependent DLS measurements with corresponding TEM images at pH 7; time-dependent TEM images at pH 3 and 4 °C, rheological strain and angular frequency sweeps, TEM images after a thermal cycle at pH 3. See DOI: 10.1039/c6py01076h

block copolymers with low polydispersities.[25] Over the past decade or so, this living radical polymerisation technique has been utilised by many research groups for the convenient synthesis of a wide range of block copolymer nanoparticles *via* polymerisation-induced self-assembly (PISA) at relatively high copolymer concentration (10–50% w/w).[26–37] In a typical PISA protocol, a macromolecular chain transfer agent (macro-CTA) is chain-extended using either RAFT emulsion polymerisation[33,34,38–41] or RAFT dispersion polymerisation.[26,35,42–45]

Self-assembly occurs *in situ* as the growing second block becomes insoluble in the reaction medium. Copolymer morphologies obtained by RAFT-mediated PISA normally depend on the relative volume fractions of the soluble and insoluble blocks, and often also on the copolymer concentration.[46] In principle, the dimensionless packing parameter, $P$, dictates the copolymer morphology. According to Israelachvili and co-workers,[47] who introduced this geometric concept for surfactant self-assembly in aqueous solution, spherical morphologies are favoured when $P \leq 1/3$. If $1/3 \leq P \leq 1/2$ then worms are obtained, while vesicles are produced when $1/2 \leq P \leq 1$. However, in practice the copolymer concentration and absolute mean degree of polymerisation of the stabiliser block often constrain the evolution in copolymer morphology during PISA, with kinetically-trapped spheres being reported in many cases (particularly for RAFT emulsion polymerisation formulations).[39,40,45,48–52] RAFT dispersion polymerisation has proved to be particularly versatile, with many robust PISA formulations being developed for both polar and non-polar solvents.[53–55] To date, end-group driven morphological transitions for block copolymer nano-objects have received relatively little attention.[56–61] There are a few reports of morphological transitions occurring as a result of end-group ionisation, but these typically involve a post-polymerisation processing step at low copolymer concentration.[56–58] In contrast, we have recently examined a prototypical PISA formulation based on the RAFT aqueous dispersion polymerisation of 2-hydroxypropyl methacrylate (HPMA) using a poly(glycerol monomethacrylate) macro-CTA in the context of end-group driven changes in copolymer morphology. For example, Lovett *et al.*[61] reported that carboxylic acid-functionalised PGMA-PHPMA chains prepared in the form of worms in concentrated acidic aqueous solution subsequently undergo an order–order transition on raising the solution pH. This causes ionisation of the carboxylic acid end-group on the PGMA stabiliser block, which leads to an increase in the relative volume fraction of the stabiliser block and hence a reduction in the packing parameter. Penfold and co-workers[59] recently reported the complementary pH-responsive behaviour for PGMA-PHPMA diblock copolymer worms prepared using a morpholine-functionalised PGMA macro-CTA. In this case, the RAFT-mediated PISA synthesis of PGMA-PHPMA worms was conducted at around pH 7 where the morpholine end-group is in its neutral form. The subsequent addition of acid led to protonation of this tertiary amine, which accordingly induced a worm-to-sphere transition.

Very recently, Lovett and co-workers reported the complex stimulus-responsive behaviour of PGMA-PHPMA vesicles when subjected to a change in solution pH.[60] More specifically, ionisation of a carboxylic acid end-group on each PGMA stabiliser block induced either a vesicle-to-worm or a vesicle-to-sphere transition, depending on the mean degree of polymerisation (DP) of the hydrophobic PHPMA block. If this DP is sufficiently high, then the additional stimulus of a reduction in temperature (from 20 °C to 4 °C) as well as a pH switch was required to induce an order–order transition. In the present study, we examine the complementary behaviour exhibited by morpholine-functionalised PGMA-PHPMA vesicles when exposed to either a pH switch, a change in temperature or both stimuli (see Scheme 1). This work differs from that recently reported by Penfold and co-workers,[59] since the initial copolymer morphology is vesicles, rather than worms.

# Experimental

## Materials

Glycerol monomethacrylate (GMA, 99.8%, ~0.06 mol% dimethacrylate impurity) was kindly donated by GEO Specialty Chemicals (Hythe, UK) and used without further purification. 2-Hydroxylpropyl methacrylate (HPMA; 97%) and 2,2′-azobis-isobutyramide dihydrochloride (AIBA; 99%) were purchased from Sigma Aldrich and were used as received. Deionised water was obtained from an Elgastat Option 3A water purification unit and ultrafiltered to remove dust using a 0.22 μm filter prior to use. All other chemicals and solvents were purchased from either VWR Chemicals or Sigma Aldrich and were used as received.

## Dynamic light scattering (DLS)

DLS studies were conducted at 20 °C using a Malvern Instruments Zetasizer Nano series instrument equipped with a 4 mW He–Ne laser ($\lambda$ = 633 nm) and an avalanche photodiode detector. Scattered light was detected at 173°. The same instrument was used for aqueous electrophoresis studies. Copolymer dispersions were diluted to 0.1% w/w using either deionised water for DLS experiments or an aqueous solution of 1 mM KCl for aqueous electrophoresis measurements. The dispersion pH was adjusted using either 0.1 M or 1 M HCl, as required. Intensity-average hydrodynamic diameters were calculated *via* the Stokes–Einstein equation, while zeta potentials were determined *via* the Henry equation using the Smoluchowski approximation. Temperature sweeps were conducted at 1 °C intervals with 10 min being allowed for thermal equilibrium at each temperature.

## Gel permeation chromatography (GPC)

Aqueous copolymer dispersions were freeze-dried overnight to obtain pale yellow powders. 0.50% w/w copolymer solutions were prepared in DMF containing DMSO (1% v/v) as a flow rate marker. GPC studies were conducted using HPLC-grade DMF eluent containing 10 mM LiBr at 60 °C at a flow rate of

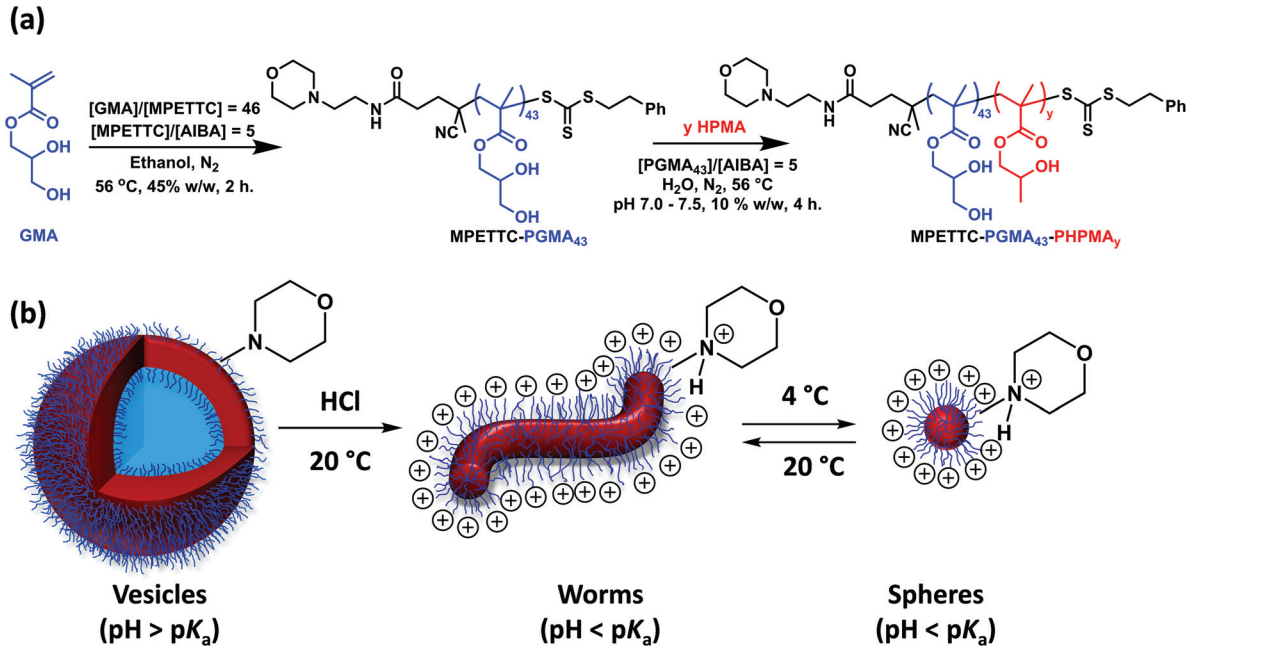


**Scheme 1** Schematic representation of (a) the synthesis of MPETTC-$PGMA_{43}$ macro-CTA by RAFT solution polymerisation of GMA and its subsequent chain extension with HPMA by RAFT aqueous dispersion polymerisation at pH 7.0–7.5 to prepare $PGMA_{43}$-$PHPMA_y$ diblock copolymer vesicles. (b) Schematic cartoon of the vesicle-to-worm transition that occurs when morpholine-functionalised $PGMA_{43}$-$PHPMA_y$ diblock copolymer vesicles undergo a pH switch on addition of acid and the reversible worm-to-sphere transition that occurs on cooling these acidified, cationic worms from 20 °C to 4 °C.

1.0 mL $min^{-1}$. A Varian 290-LC pump injection module was connected to two Polymer Laboratories 5 μm PL gel Mixed-C columns connected in series and a Varian 390-LC multi-detector suite (only the refractive index detector was used). Sixteen near-monodisperse poly(methyl methacrylate) standards ranging from $M_p$ = 645 g $mol^{-1}$ to 2 480 000 g $mol^{-1}$ were used for column calibration.

### $^1$H NMR spectroscopy

$^1$H NMR spectra were recorded at 298 K using a 400 MHz Bruker AV3-HD spectrometer in $CD_3OD$. Sixty-four scans were averaged per spectrum and all chemical shifts are reported in ppm ($\delta$).

### Transmission electron microscopy (TEM)

Copper/palladium grids were coated with a thin film of amorphous carbon, then subjected to a plasma glow discharge for 30 seconds to produce a hydrophilic surface. Aqueous copolymer dispersions were diluted from 10% to 0.1% w/w solids at either pH 7 or pH 3. An aqueous droplet (10 μL) of a 0.1% w/w copolymer dispersion at the desired pH and temperature was placed on a hydrophilic grid for 40 seconds and blotted to remove excess solution. Each grid was negatively stained using uranyl formate (0.75% w/v) solution for 20 seconds. Excess stain was removed by blotting and each grid was carefully dried with a vacuum hose. TEM images were recorded using a FEI Tecnai Spirit instrument fitted with an Orius SC1000B camera operating at 80 kV.

### Rheology

An AR-G2 rheometer equipped with a variable temperature Peltier plate and a 40 mm 2° aluminium cone was used for all rheological experiments. Percentage strain sweeps were conducted at an angular frequency of 1.0 rad $s^{-1}$ and angular frequency sweeps were conducted at 1.0% strain; these conditions correspond to the viscoelastic regime. Both percentage strain and angular frequency sweeps were conducted on diblock copolymer worm gels at pH 3 and 20 °C. The storage ($G'$) and loss ($G''$) moduli were determined for a 10% w/w aqueous copolymer dispersion as a function of temperature using the above conditions, with an equilibration time of 20 min being allowed for each 1 °C increment.

### Turbidimetry

The absorbance of 0.1% w/w aqueous diblock copolymer dispersions was recorded using a Shimadzu UV-1800 spectrometer operating at 450 nm and 20 °C. The solution pH was adjusted to pH 7, 3 or 1, with additional studies being performed at pH 3 in the presence of 100 mM KCl.

### Synthesis of MPETTC-poly(glycerol monomethacrylate) macro-CTA by RAFT solution polymerisation in ethanol

MPETTC RAFT agent was prepared as described previously.[59] A 100 ml round-bottom flask was charged with a magnetic stirrer bar, glycerol monomethacrylate (GMA, 18.5 g, 116 mmol), MPETTC RAFT agent (1.16 g, 2.57 mmol; target DP = 45), AIBA (0.139 g, 0.51 mmol; [MPETTC]/[AIBA] molar

 

ratio = 5.0) and ethanol (24.2 g) to afford a 45% w/w orange solution. The flask was sealed, placed in an ice bath and degassed under $N_2$ for 30 min, before being placed in a pre-heated oil bath set at 56 °C. The GMA polymerisation was allowed to proceed for 2 h at this temperature, then quenched by cooling to 20 °C with concomitant exposure to air. $^1$H NMR studies indicated 72% GMA conversion (the integrated aromatic end-group signals at $\delta$ 7.1–7.4 were compared to the vinyl signals at $\delta$ 6.14–6.20). Purification was achieved by precipitation into a twenty-fold excess of dichloromethane to remove unreacted GMA monomer, followed by filtration. The crude PGMA was redissolved in the minimum amount of methanol and precipitated a second time using a ten-fold excess dichloromethane, with isolation achieved *via* filtration. Purified PGMA macro-CTA was dissolved in water, placed on a rotary evaporator to remove residual dichloromethane, and then freeze-dried for 48 h to afford a yellow powder. $^1$H NMR studies confirmed the absence of residual GMA monomer.

### Synthesis of MPETTC-poly(glycerol monomethacrylate)-poly(2-hydroxypropyl methacrylate) diblock copolymer vesicles by RAFT aqueous dispersion polymerisation of HPMA

A typical protocol for the synthesis of MPETTC-PGMA$_{43}$-PHPMA$_{200}$ diblock copolymer vesicles by RAFT aqueous dispersion polymerisation of HPMA was as follows. PGMA$_{43}$ macro-CTA (0.40 g, 54.5 μmol), HPMA monomer (1.57 g, 10.9 mmol; target DP = 200), AIBA (2.95 mg, 10.8 μmol; [PGMA$_{43}$]/[AIBA] molar ratio = 5.0) and $H_2O$ (17.85 mL) were added to a 24 mL sample vial fitted with a suba-seal to afford a 10% w/w reaction solution. The solution pH was adjusted to pH 7.0–7.5 using 0.1 M KOH, if required. The reaction flask was sealed, placed in an ice bath and degassed using a $N_2$ gas stream for 30 min, then placed in a preheated oil bath set at 56 °C. The HPMA polymerisation was allowed to proceed at this temperature for 4 h, then quenched by exposure to air while cooling to 20 °C. Alternative DPs for the PHPMA block were targeted by simply varying the number of moles of HPMA in the formulation (adjusting the amount of water to maintain the same overall 10% w/w solids concentration) to produce four diblock copolymer vesicle dispersions, whose aqueous solution behaviour was assessed by $^1$H NMR, DLS, DMF GPC, TEM, turbidimetry and rheological studies.

## Results and discussion

### Synthesis of morpholine-functionalised PGMA$_{43}$-PHPMA$_y$ vesicles

A morpholine-functionalised PGMA macro-CTA was successfully prepared by the RAFT solution polymerisation of GMA using MPETTC in ethanol, as recently reported.[62] $^1$H NMR studies enabled a mean DP of 43 to be calculated *via* end-group analysis by comparing the integrated aromatic end-group signals at 7.2–7.4 ppm to that of the methacrylic backbone at 0–2.5 ppm. DMF GPC studies indicated an $M_n$ of 12 700 g mol$^{-1}$ and $M_w/M_n$ of 1.13 (see Fig. 1). This water-soluble MPETTC-PGMA$_{43}$ macro-CTA was subsequently chain-extended with HPMA at 56 °C using a RAFT aqueous dispersion polymerisation formulation to generate a series of four MPETTC-PGMA$_{43}$-PHPMA$_y$ diblock copolymer vesicles ($y$ = 190, 200, 220 or 230) at 10% w/w solids. The p$K_a$ of the morpholine end-group of a near-identical MPETTC-PGMA$_{50}$ macro-CTA was recently determined to be approximately 6.3.[59] Consequently, the pH was adjusted to between 7.0–7.5 prior to the HPMA polymerisation to ensure that most of the morpholine end-groups of the MPETTC-PGMA$_{43}$-PHPMA$_y$ diblock copolymer chains were present in their neutral free amine form. A higher solution pH was not investigated because it is well-known that alkaline conditions lead to premature hydrolysis of the RAFT CTA chain-ends.[62–64] Monomer conversions were estimated to be more than 99% by $^1$H NMR spectroscopy. DMF GPC indicated high blocking efficiencies for the MPETTC-PGMA$_{43}$ macro-CTA and relatively narrow molecular weight distributions for the resulting MPETTC-PGMA$_{43}$-PHPMA$_y$ diblock copolymers (see Fig. 1). TEM studies confirmed the presence of polydisperse vesicles for all four diblock copolymer compositions prepared at pH 7.0, with number-average diameters ranging from 150 to 450 nm (Fig. 2A). Initial experiments confirmed that a diblock copolymer with a slightly lower core-forming block DP (MPETTC-PGMA$_{43}$-PHPMA$_{180}$) formed a vesicle/worm mixed phase, rather than pure vesicles. Thus the vesicles prepared for this study clearly lie close to the vesicle/worm phase boundary.

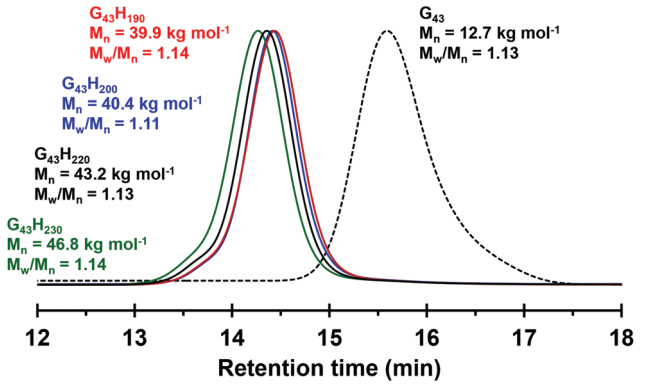


Fig. 1 DMF chromatograms obtained for MPETTC-PGMA$_{43}$ macro-CTA (black dotted curve) and the corresponding MPETTC-PGMA$_{43}$-PHPMA$_y$ diblock copolymer vesicles ($y$ = 190, 200, 220 and 230). Molecular weight data are calculated relative to a series of near-monodisperse poly(methyl methacrylate) calibration standards. G and H denote poly(glycerol monomethacrylate) and poly(2-hydroxypropyl methacrylate), respectively.

### pH-Responsive behaviour of MPETTC-PGMA$_{43}$-PHPMA$_y$ vesicles

The solution pH for all four 10% w/w vesicle dispersions was adjusted to pH 3.0 using 1 M HCl. For a PHPMA DP of either

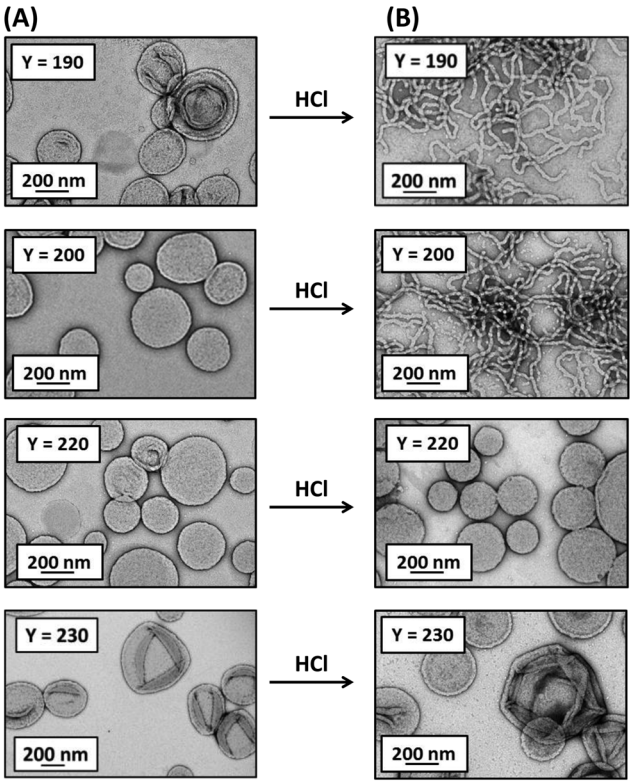


Fig. 2 Transmission electron microscopy images obtained for 0.1% w/w aqueous dispersions of MPETTC-PGMA$_{43}$-PHPMA$_y$ ($y$ = 190, 200, 220 and 230) diblock copolymer nanoparticles at either (A) pH 7.0 or (B) pH 3.0. The pH switch was performed at 20 °C at 10% w/w copolymer concentration in each case.

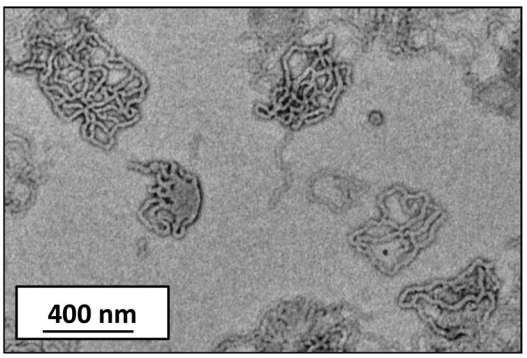


Fig. 3 Representative TEM image obtained for the transient 'jellyfish' intermediate structures formed by an MPETTC-PGMA$_{43}$-PHPMA$_{190}$ diblock copolymer after 24 h at pH 3.0.

190 or 200, a change in the aqueous dispersion appearance from a free-flowing turbid fluid to a semi-translucent free-standing gel was observed 48 h after lowering the pH (Fig. S1†). This change in physical appearance is consistent with a vesicle-to-worm transition. However, free-flowing turbid fluids were obtained both before and after lowering the solution pH for a PHPMA DP of 220 or 230. TEM studies on the acidified aqueous dispersions confirmed a pure worm copolymer morphology for PHPMA DPs of 190 and 200, but no change in morphology was observed for the two higher PHPMA DPs (Fig. 2B).

The vesicle-to-worm transition observed for $y$ = 190 or 200 is in good agreement with a complementary report recently reported by our group[60] and occurs because the morpholine group located at the end of the PGMA stabiliser becomes fully protonated at pH 3.0. This leads to a subtle increase in the volume fraction of this hydrophilic block, which in turn lowers the packing parameter, $P$, from the vesicle regime ($1/2 \leq P \leq 1$) to the worm regime ($1/3 \leq P \leq 1/2$).[46]

The vesicle-to-worm transition is significantly slower than the corresponding worm-to-sphere transition, with 48 h being required in the former case. Interestingly, jellyfish-like structures are observed by TEM after 24 h (Fig. 3). This suggests that the mechanism for the vesicle-to-worm transition is closely related to that for the worm-to-vesicle transition previously reported by Blanazs and co-workers.[65] However, on returning to pH 7 an inhomogeneous white paste is formed, which undergoes syneresis (phase separation) within minutes. Heating to 56 °C for 24 h did not lead to redispersion. These observations indicate the irreversible nature of this pH-triggered vesicle-to-worm transition (Fig. S1†). We suspect that this irreversible behaviour is because of the lack of HPMA monomer, which acts as a co-solvent for the PHPMA core-forming block during the PISA synthesis of the initial vesicles. When the core-forming block is increased to a PHPMA DP of 220 or 230, protonation of the morpholine end-groups is insufficient to induce a change in the packing parameter to favour the worm phase. This is expected, as increasing the PHPMA DP increases the packing parameter, so the vesicles lie further from the worm/vesicle boundary. Thus the modest increase in stabiliser volume fraction cannot induce a morphological transition. It is perhaps noteworthy that, for an intermediate $y$ value of 210, a morphology change from vesicles to a vesicle/worm mixed phase occurs on acidification to pH 3.0, as judged by TEM (Fig. S2†). However, this block composition is not discussed further in this study.

Dynamic light scattering and aqueous electrophoresis studies were conducted on MPETTC-PGMA$_{43}$-PHPMA$_y$ vesicles at 20 °C to examine the effect of varying the solution pH on the mean particle diameter and zeta potential (Fig. 4). Diblock copolymer vesicles were diluted to 0.1% w/w and the pH was adjusted using 1 M or 0.1 M. These diluted dispersions were left for 48 h in a 20 °C incubator to ensure that equilibrium morphologies were attained. Where a vesicle-to-worm transition was observed, a significant reduction in apparent particle diameter was observed [from 415 nm to 135 nm for $y$ = 190 or from 392 nm to 196 nm for $y$ = 200], with a corresponding increase in zeta potential from −14 mV to +22 mV ($y$ = 190) and −13 mV to +25 mV ($y$ = 200) occurring on lowering the dispersion pH from 7.1 to 3.0 (Fig. 4a and b).

Intensity-average hydrodynamic diameters were calculated *via* the Stokes–Einstein equation, hence a 'sphere-equivalent' diameter is reported for the worms, which corresponds to

 

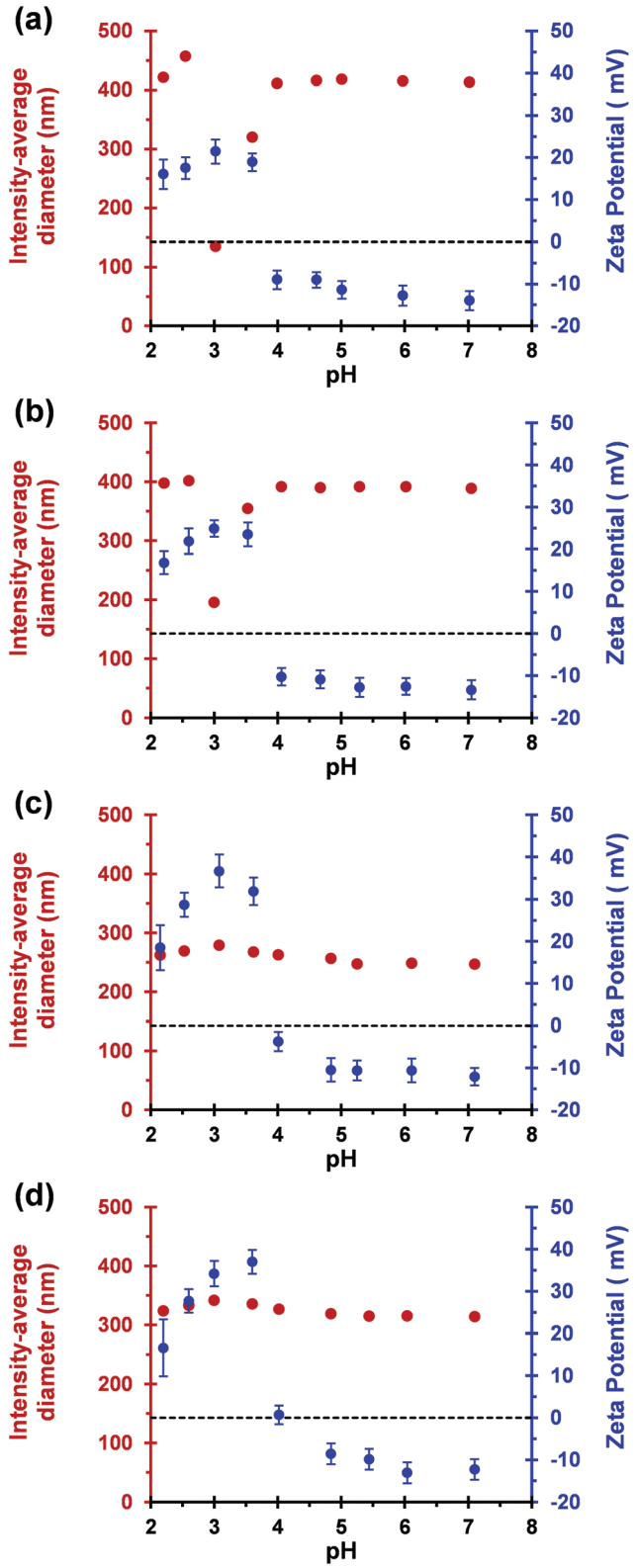


Fig. 4 Intensity-average diameter *vs.* pH and zeta potential *vs.* pH curves obtained for MPETTC-PGMA$_{43}$-PHPMA$_y$ diblock copolymer nano-objects where $y$ = (a) 190, (b) 200, (c) 220 and (d) 230. All measurements were made at 20 °C for 0.1% w/w copolymer dispersions prepared in the presence of 1 mM KCl background salt.

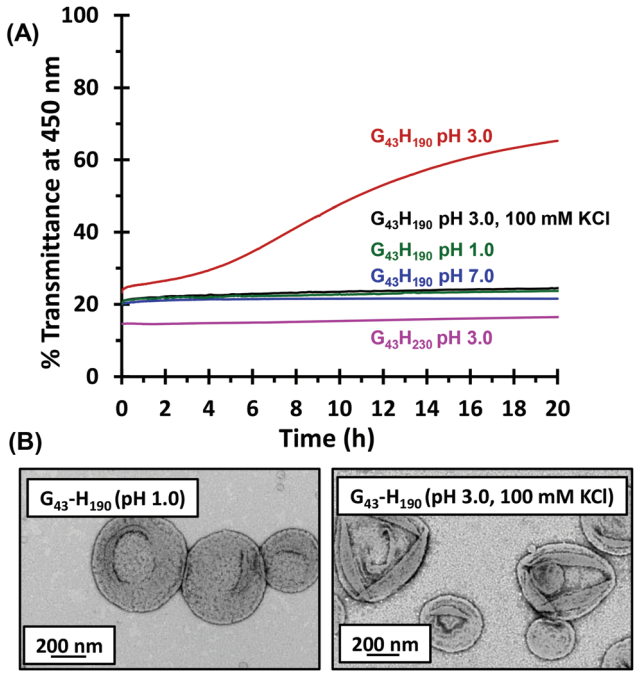


Fig. 5 (a) Turbidimetric data obtained for MPETTC-PGMA$_{43}$-PHPMA$_{190}$ nano-objects at either pH 7.0, pH 3.0 or pH 1.0, or at pH 3.0 in the presence of 100 mM KCl, for (non-responsive) MPETTC-PGMA$_{43}$-PHPMA$_{230}$ vesicles. All measurements were recorded over 20 h for 0.1% w/w dispersions at 20 °C. (b) TEM images obtained for MPETTC-PGMA$_{43}$-PHPMA$_{190}$ diblock copolymer vesicles after 20 h at either pH 1.0 in the absence of added salt or pH 3.0 in the presence of 100 mM KCl. This confirms that the original vesicle morphology is retained under these conditions.

neither the mean worm length nor the mean worm width. This reduction in nanoparticle dimensions and surface charge reversal is consistent with TEM studies and provides strong evidence that a pure phase of cationic worms is formed at pH 3.0. Below this pH, the apparent particle diameter increases further to 457 nm ($y$ = 190) and 415 nm ($y$ = 200), while the corresponding zeta potentials are reduced as excess HCl screens the cationic surface charge arising from the protonated morpholine end-groups. According to DLS (and TEM; see Fig. 5) studies, the initial vesicular morphology remains unperturbed under these conditions. The modest increase in vesicle diameter below pH 3.0 is the result of the protonated morpholine end-groups inducing an increase in hydration (and hence thickness) for the PGMA$_{43}$ stabiliser block. In this case no morphology transition occurs because the excess acid acts as background salt, thus screening the cationic end-group.

For block copolymer compositions for which no morphological transition was observed even at the optimal pH of 3.0 ($y$ = 220 and 230), a modest increase in hydrodynamic diameter of approximately 30 nm occurred on lowering the dispersion pH from 7.1 to 3.0. A simultaneous change in zeta potential from approximately −10 mV to +35 mV occurs (Fig. 4c and d). Furthermore, the zeta potential for these cat-

ionic vesicles is greater than that reported for the cationic worms at pH 3.0 (+35 mV *vs.* + 25 mV). We note that Ohshima has recently published an approximate analytical expression for the electrophoretic mobility of cylindrical colloidal particles.[66] However, this refinement has not been utilised in the present study. Like the two diblock copolymer compositions for which a vesicle-to-worm transition was observed, the zeta potential of these cationic vesicles was reduced below pH 3.0 because excess HCl acted as a salt, leading to charge screening.

Diblock copolymer vesicles typically appear turbid because they are relatively large and hence strongly scatter visible light. In contrast, worms scatter light rather less efficiently. Hence a turbidimetry study was conducted whereby the transmittance of light at an arbitrary wavelength of 450 nm was monitored over 20 h to examine the time scale required for the MPETTC-PGMA$_{43}$-PHPMA$_{190}$ vesicle-to-worm transition. Diblock copolymer dispersions were diluted to 0.1% w/w so the transmittance was within the appropriate range. At pH 7.0, the transmittance recorded for the vesicles remained essentially unchanged over 20 h (Fig. 5a, blue trace). However, when these vesicles were diluted to pH 3.0, a gradual increase in transmittance was observed over time, indicating a vesicle-to-worm transition. Moreover, this order–order transition was very sensitive to the presence of electrolyte. Essentially no change in transmittance occurred after 20 h either at pH 1.0 (where excess HCl acts as a salt) or at pH 3.0 in the presence of 100 mM KCl; TEM studies confirmed the presence of a pure vesicle phase in both cases (Fig. 5b). Conversely, if MPETTC-PGMA$_{43}$-PHPMA$_{230}$ vesicles are examined at pH 3.0, the transmittance remains essentially unchanged over 20 h because protonation of the morpholine end-groups is not sufficient to induce a morphological transition owing to the relatively long core-forming block.

### Thermoresponsive behaviour of MPETTC-PGMA$_{43}$-PHPMA$_y$ vesicles

The thermoresponsive behaviour of PGMA-PHPMA diblock copolymer worm gels has been studied in great detail by Armes and co-workers.[67–69] It is well-established that a thermo-reversible worm-to-sphere transition (with concomitant degelation) occurs on cooling to 4 °C as the weakly hydrophobic PHPMA cores become more hydrated at lower temperatures. However, further cooling to −2 °C resulted in almost complete molecular dissolution of PGMA-PHPMA diblock copolymer chains.[69] In the present study, the focus is on order–order transitions rather than order–disorder transitions, so the lower temperature limit was set to 4 °C. In addition, Verber *et al.* found that the critical gelation temperature (CGT) of PGMA$_{54}$-PHPMA$_y$ worms ($y$ = 130 to 170) could be lowered by targeting progressively longer PHPMA DPs. This is because the hydrophobic core required a greater degree of hydration, and hence a lower temperature, in order to induce a morphological transition.[68] Temperature-dependent studies conducted on carboxylic acid-terminated PGMA$_{43}$-PHPMA$_y$ diblock copolymer vesicles have been reported by Lovett and co-workers who only observed thermo-responsive behaviour for a PHPMA DP of 170.[60] Thus DLS and TEM were used to examine the thermo-responsive behaviour for all four MPETTC-PGMA$_{43}$-PHPMA$_y$ diblock copolymer vesicles on cooling from 25 °C to 4 °C (Fig. S3†). All DLS measurements were conducted at pH 7.0 in order to exclude any effect of the morpholine end-group. In each case, no significant change in either the intensity-average diameter or the polydispersity index was observed on cooling. These observations are in good agreement with those reported by Lovett *et al.*[60] If a vesicle-to-worm transition had occurred on cooling, a reduction in apparent particle diameter and a concomitant significant increase in polydispersity index would be expected. These results are in good agreement with TEM studies, which confirmed that no change in copolymer morphology occurred on cooling to 4 °C. Thus, for this mini-series of MPETTC-PGMA$_{43}$-PHPMA$_y$ vesicles, end-group ionisation seems to be a more powerful stimulus for inducing a morphology transition than temperature.

### Dual-stimulus behaviour of MPETTC-PGMA$_{43}$-PHPMA$_y$ vesicles

All four MPETTC-PGMA$_{43}$-PHPMA$_y$ diblock copolymer nano-objects obtained at pH 3 were cooled from 20 °C to 4 °C in order to examine the dual-stimulus effect of both pH and temperature on the copolymer morphology. DLS temperature sweeps were conducted from 25 °C to 4 °C with 10 min being allowed at each temperature for thermal equilibration; subsequent TEM studies were conducted on 0.1% w/w dispersions dried at 4 °C (Fig. 6).

When the PHPMA DP is 190, 200 or 220 (Fig. 6a–c), DLS studies indicated a significant reduction in intensity-average diameter to approximately 50 nm at 4 °C, with much lower scattered light intensities (or derived count rates). These observations suggest that a change in morphology from either vesicles to spheres or worms to spheres occurs. The mean zeta potential for these spheres at pH 3 is +23 mV at 4 °C. However, no reduction in intensity-average diameter on cooling was observed for a PHPMA DP of 230. TEM studies indicated the presence of vesicles comprising a distinctive worm-like surface texture and a diameter of approximately 300–400 nm, which is consistent with the intensity-average diameter of 328 nm reported by DLS. A similar morphology has been observed by Förster and co-workers[70] for poly(ethylene oxide)–poly(2-vinylpyridine) vesicles subjected to cooling from 25 °C to 4 °C. Cryo-TEM studies revealed a 'basket-like network of worm-like micelles' after 1 h, which eventually dissociated into isolated worms after 24 h. Similarly, after ageing the MPETTC-PGMA$_{43}$-PHPMA$_{230}$ dispersion for 24 h at 4 °C, TEM studies confirmed that the surface-textured vesicles shown in Fig. 6d broke up to form a mixed phase comprising spheres and worms (Fig. S4a†). Moreover, when the original diblock copolymer vesicles were exposed to a dual temperature plus pH stimulus at 10% w/w copolymer concentration, the same change in morphology is observed by TEM (after dilution to 0.1% w/w prior to analysis) (Fig. S4b†). Hence such transitions are clearly not merely a dilution artefact.

 

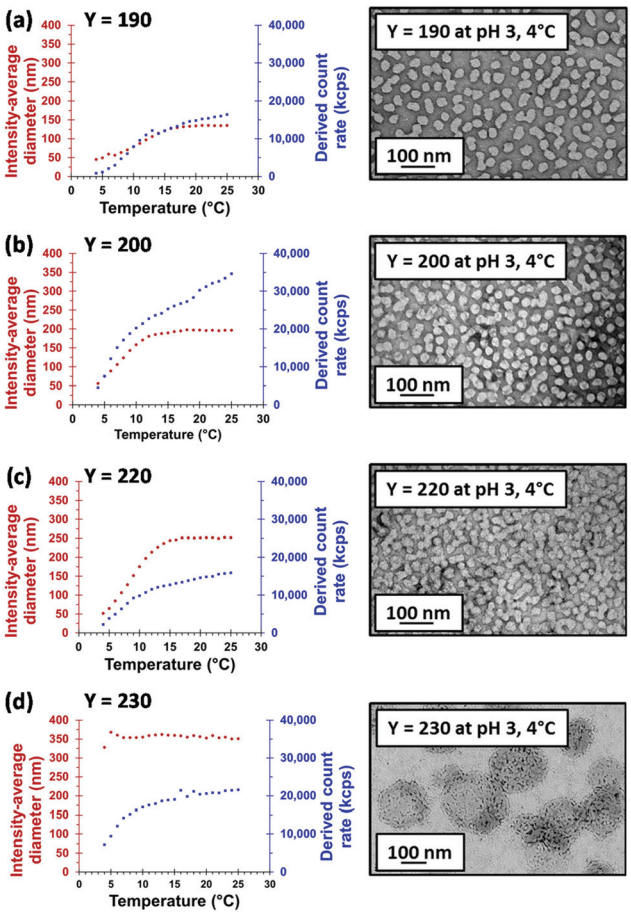


Fig. 6 Variation in intensity-average diameter and derived count rate *vs.* temperature on cooling a 0.1% w/w aqueous dispersion of MPETTC-PGMA$_{43}$-PHPMA$_y$ diblock copolymer nano-objects at pH 3 from 20 °C to 4 °C and the corresponding TEM images obtained on drying at 4 °C for *y* values of (a) 190, (b) 200, (c) 220 and (d) 230.

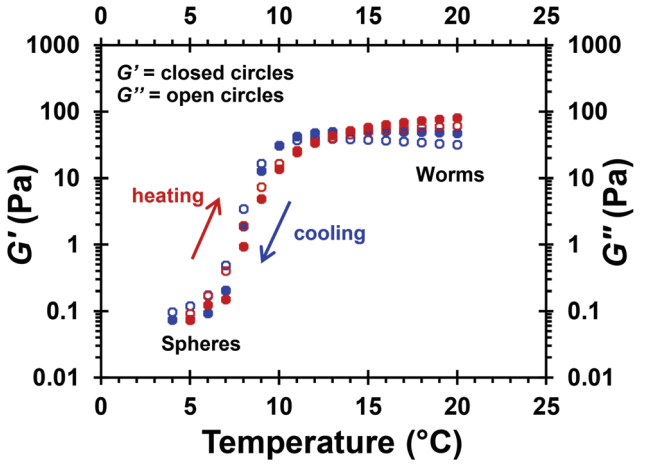


Fig. 7 Variation of storage modulus (*G′*, filled circles) and loss modulus (*G″*, open circles) with temperature for a 10% w/w aqueous dispersion of MPETTC-PGMA$_{43}$-PHPMA$_{190}$ diblock copolymer worms at pH 3. The blue circles represent a cooling cycle from 20 °C to 4 °C and the red circles represent a heating cycle from 4 °C to 20 °C. Measurements were conducted at an angular frequency of 1.0 rad s$^{-1}$ and an applied strain of 1.0%, with an equilibration time of 20 min at each temperature.

Temperature-dependent oscillatory rheology studies were performed on a 10% w/w aqueous dispersion of MPETTC-PGMA$_{43}$-PHPMA$_{190}$ worms at pH 3. Angular frequency and percentage strain sweeps indicated the formation of a viscoelastic gel at 20 °C using an angular frequency of 1.0 rad s$^{-1}$ and an applied strain of 1.0% (Fig. S5†). These conditions were then used to perform a temperature sweep from 20 °C to 4 °C to 20 °C (Fig. 7). An initial gel strength of 47 Pa was observed at 20 °C. This gel strength is lower than that indicated in previous reports for the same copolymer concentration.[67,68] This is attributed to the cationic surface charge leading to weak electrostatic repulsion between neighbouring worms, thus reducing the number of inter-worm contacts. A worm-to-sphere transition occurred on cooling to 4 °C, which leads to *in situ* degelation (see Fig. 6a). A critical gelation temperature (CGT) of 10 °C was observed, as judged by the cross-over temperature for the G′ and G″ curves. This is marginally higher than that reported by Verber *et al.*,[68] which we attribute to the greater hydration of the cationic PGMA$_{43}$ stabiliser at pH 3 compared to the neutral PGMA$_{43}$ chains at pH 7. Regelation occurred at 12 °C during heating from 4 °C to 20 °C, with minimal hysteresis being observed. However, a somewhat stronger gel (G′ = 80 Pa) was obtained on returning to 20 °C. TEM confirmed the presence of diblock copolymer worms under these conditions (Fig. S6†). However, DLS studies indicated a sphere-equivalent diameter of 148 nm for the reconstituted worms after the temperature cycle, which is marginally larger than that obtained before the thermal cycle (135 nm). Thus we attribute the observed increase in gel strength to a longer mean worm contour length and hence a greater number of inter-worm contacts. This observation is strikingly different to that reported by Lovett *et al.*, who observed an irreversible worm-to-sphere for carboxylic acid-functionalised PGMA-PHPMA worms subjected to a similar thermal cycle.[60] However, this difference might be simply the result of the rather longer equilibration time of 20 min (*vs.* 2 min (ref. 60)) employed for the gel rheology experiments in the current study.

Clearly, the stimulus-responsive behaviour of MPETTC-PGMA$_{43}$-PHPMA$_y$ vesicles is remarkably complex, as summarised in Table 1. Protonation of a single morpholine end-group located at the end of the PGMA stabiliser block induces a subtle increase in its volume fraction. This in turn leads to a reduction in the packing parameter, which drives a vesicle-to-worm transition. Lowering the solution temperature increases the degree of hydration of the PHPMA core-forming block, which further reduces the packing parameter and hence leads to the formation of spheres. Warming these spheres induces a sphere-to-worm transition as the PHPMA cores gradually become less solvated, hence increasing the packing parameter. However, if the PHPMA DP is too high then protonation of the morpholine end-group alone is not sufficient enough to

Table 1 Summary of observations made for four MPETTC-PGMA$_{43}$-PHPMA$_y$ diblock copolymer vesicles illustrating their pH-responsive, thermo-responsive and dual stimulus-responsive behaviour

| | | Morphology observed by TEM under the stated conditions | | | | Summary of stimulus-responsive behaviour | | |
|---|---|---|---|---|---|---|---|---|
| Target PHPMA DP | $M_n$/kg mol$^{-1}$ ($M_w/M_n$)[a] | pH 7 [b] | pH 3 [b] | pH 3 + 100 mM KCl or pH 1 (no salt)[b] | pH 3 [c] | pH-responsive? | Thermo-responsive? | pH- and thermo-responsive? |
| 190 | 39.9 (1.14) | Vesicles | Worms | Vesicles | Spheres | Yes | No | Yes |
| 200 | 40.4 (1.11) | Vesicles | Worms | Vesicles | Spheres | Yes | No | Yes |
| 220 | 43.2 (1.13) | Vesicles | Vesicles | Vesicles | Spheres | No | No | Yes |
| 230 | 46.8 (1.14) | Vesicles | Vesicles | Vesicles | Spheres & worms | No | No | Yes |

[a] Determined by DMF GPC *vs.* PMMA standards. [b] Particle morphology determined by TEM at 20 °C. [c] Particle morphology determined by TEM at 4 °C.

drive a morphological transition. Nevertheless, the application of both pH and temperature stimuli results in an overall vesicle-to-sphere or vesicle-to-sphere/short worm morphological transition (depending on the precise PHPMA DP) by increasing the effective PGMA stabiliser volume fraction and the degree of hydration of the core-forming PHPMA block, respectively. These pH-responsive vesicles are currently being investigated for the *in situ* encapsulation and subsequent pH-triggered release of model nanoparticles such as ultrafine aqueous silica sols and globular proteins.[71]

## Conclusions

In summary, a water-soluble MPETTC-PGMA$_{43}$ macro-CTA was chain-extended with HPMA to form a series of four MPETTC-PGMA$_{43}$-PHPMA$_y$ diblock copolymer vesicles at 10% w/w solids at approximately neutral pH. Acidification to pH 3 leads to protonation of the morpholine end-group and consequently induces a change in copolymer morphology from weakly anionic vesicles to a pure phase comprising cationic worms for $y$ values of 190 or 200. The presence of added electrolyte (excess HCl at pH 1 or 100 mM KCl) causes charge-screening, which suppresses this order–order transition. Turbidimetry studies confirm that such vesicle-to-worm transitions are relatively slow compared to the worm-to-sphere transition previously reported.[59] Moreover, no change in morphology is observed for higher PHPMA DPs, because this membrane-forming block becomes too hydrophobic to be affected by this rather subtle end-group effect. The series of four MPETTC-PGMA$_{43}$-PHPMA$_y$ vesicles reported herein did not exhibit thermoresponsive behaviour when cooled to 4 °C at neutral pH. However, lowering both the solution pH and temperature induced a vesicle-to-sphere transition (or a mixture of spheres and short worms, depending on the PHPMA DP). Nevertheless, vesicles comprising the longest PHPMA block ($y$ = 230) responded much more slowly to this dual stimulus. Temperature-dependent gel rheology studies conducted on acidified MPETTC-PGMA$_{43}$-PHPMA$_{190}$ worms at pH 3 confirmed that the worm-to-sphere transition is fully reversible. In summary, the aqueous solution behaviour of MPETTC-PGMA$_{43}$-PHPMA$_y$ vesicles is rather complex and critically depends on the PHPMA DP, the solution pH and temperature. This study provides useful new insights regarding the pH-responsive behaviour of non-ionic vesicles modulated by morpholine end-groups located on the stabiliser block.

## Conflict of interest

The authors declare no competing financial interest.

## Acknowledgements

ESPRC and P & G (Brussels) are thanked for supporting a CASE PhD studentship for NJWP. SPA acknowledges an ERC Advanced Investigator grant (PISA 320372). Dr Svetomir Tzokov is thanked for carbon coating the TEM grids.

## Notes and references

1 L. Zhang and A. Eisenberg, *Science*, 1995, **268**, 1728.
2 K. Yu and A. Eisenberg, *Macromolecules*, 1996, **29**, 6359.
3 D. J. Pochan, Z. Chen, H. Cui, K. Hales, K. Qi and K. L. Wooley, *Science*, 2004, **306**, 94.
4 B. M. Discher, Y.-Y. Won, D. S. Ege, J. C. M. Lee, F. S. Bates, D. E. Discher and D. A. Hammer, *Science*, 1999, **284**, 1143.
5 J. C. M. Lee, H. Bermudez, B. M. Discher, M. A. Sheehan, Y.-Y. Won, F. S. Bates and D. E. Discher, *Biotechnol. Bioeng.*, 2001, **73**, 135.
6 D. E. Discher and A. Eisenberg, *Science*, 2002, **297**, 967.
7 H. Bermudez, A. K. Brannan, D. A. Hammer, F. S. Bates and D. E. Discher, *Macromolecules*, 2002, **35**, 8203.
8 R. C. Hayward and D. J. Pochan, *Macromolecules*, 2010, **43**, 3577.
9 F. Liu and A. Eisenberg, *J. Am. Chem. Soc.*, 2003, **125**, 15059.
10 D. M. Vriezema, M. C. Aragones, J. A. A. W. Elemans, J. J. L. M. Cornelissen, A. E. Rowan and R. J. M. Nolte, *Chem. Rev.*, 2005, **105**, 1445.
11 C. Lo Presti, H. Lomas, M. Massignani, T. Smart and G. Battaglia, *J. Mater. Chem.*, 2009, **19**, 3576.

 

12 C. J. Mable, N. J. Warren, K. L. Thompson, O. O. Mykhaylyk and S. P. Armes, *Chem. Sci.*, 2015, **6**, 6179.
13 B. Surnar and M. Jayakannan, *Biomacromolecules*, 2013, **14**, 4377.
14 J. Du, L. Fan and Q. Liu, *Macromolecules*, 2012, **45**, 8275.
15 H. Xu, F. Meng and Z. Zhong, *J. Mater. Chem.*, 2009, **19**, 4183.
16 J. Du, Y. Tang, A. L. Lewis and S. P. Armes, *J. Am. Chem. Soc.*, 2005, **127**, 12800.
17 K. E. B. Doncom, C. F. Hansell, P. Theato and R. K. O'Reilly, *Polym. Chem.*, 2012, **3**, 3007.
18 E. Blasco, J. L. Serrano, M. Pinol and L. Oriol, *Macromolecules*, 2013, **46**, 5951.
19 J. He, P. Zhang, T. Babu, Y. Liu, J. Gong and Z. Nie, *Chem. Commun.*, 2013, **49**, 576.
20 K. Yu and A. Eisenberg, *Macromolecules*, 1998, **31**, 3509.
21 J. Du and R. K. O'Reilly, *Macromol. Chem. Phys.*, 2010, **211**, 1530.
22 A. E. Smith, X. Xu, S. E. Kirkland-York, D. A. Savin and C. L. McCormick, *Macromolecules*, 2010, **43**, 1210.
23 A. Feng, C. Zhan, Q. Yan, B. Liu and J. Yuan, *Chem. Commun.*, 2014, **50**, 8958.
24 J. Chiefari, Y. K. Chong, F. Ercole, J. Krstina, J. Jeffery, T. P. T. Le, R. T. A. Mayadunne, G. F. Meijs, C. L. Moad, G. Moad, E. Rizzardo and S. H. Thang, *Macromolecules*, 1998, **31**, 5559.
25 G. Moad, E. Rizzardo and S. H. Thang, *Aust. J. Chem.*, 2009, **62**, 1402.
26 S. Sugihara, S. P. Armes, A. Blanazs and A. L. Lewis, *Soft Matter*, 2011, **7**, 10787.
27 Y. Pei and A. B. Lowe, *Polym. Chem.*, 2014, **5**, 2342.
28 J. Rieger, C. Grazon, B. Charleux, D. Alaimo and C. Jerome, *J. Polym. Sci., Part A: Polym. Chem.*, 2009, **47**, 2373.
29 M. Williams, N. J. W. Penfold and S. P. Armes, *Polym. Chem.*, 2016, **7**, 384.
30 Y. Pei, O. R. Sugita, L. Thurairajah and A. B. Lowe, *RSC Adv.*, 2015, **5**, 17636.
31 Y. Pei, L. Thurairajah, O. R. Sugita and A. B. Lowe, *Macromolecules*, 2015, **48**, 236.
32 X. Zhang, S. Boisse, C. Bui, P.-A. Albouy, A. Brulet, M.-H. Li, J. Rieger and B. Charleux, *Soft Matter*, 2012, **8**, 1130.
33 X. Zhang, S. Boisse, W. Zhang, P. Beaunier, F. D'Agosto, J. Rieger and B. Charleux, *Macromolecules*, 2011, **44**, 4149.
34 S. Boisse, J. Rieger, K. Belal, A. Di-Cicco, P. Beaunier, M.-H. Li and B. Charleux, *Chem. Commun.*, 2010, **46**, 1950.
35 Y. Ning, L. A. Fielding, K. E. B. Doncom, N. J. W. Penfold, A. N. Kulak, H. Matsuoka and S. P. Armes, *ACS Macro Lett.*, 2016, **5**, 311.
36 M. Semsarilar, N. J. W. Penfold, E. R. Jones and S. P. Armes, *Polym. Chem.*, 2015, **6**, 1751.
37 M. Williams, N. J. W. Penfold, J. R. Lovett, N. J. Warren, C. W. I. Douglas, N. Doroshenko, P. Verstraete, J. Smets and S. P. Armes, *Polym. Chem.*, 2016, **7**, 3864.
38 M. F. Cunningham, *Prog. Polym. Sci.*, 2008, **33**, 365.
39 V. J. Cunningham, A. M. Alswieleh, K. L. Thompson, M. Williams, G. J. Leggett, S. P. Armes and O. M. Musa, *Macromolecules*, 2014, **47**, 5613.
40 W. Zhang, F. D'Agosto, O. Boyron, J. Rieger and B. Charleux, *Macromolecules*, 2012, **45**, 4075.
41 W. Zhang, F. D'Agosto, O. Boyron, J. Rieger and B. Charleux, *Macromolecules*, 2011, **44**, 7584.
42 P. Shi, Q. Li, X. He, S. Li, P. Sun and W. Zhang, *Macromolecules*, 2014, **47**, 7442.
43 N. J. Warren, O. O. Mykhaylyk, A. J. Ryan, M. Williams, T. Doussineau, P. Dugourd, R. Antoine, G. Portale and S. P. Armes, *J. Am. Chem. Soc.*, 2015, **137**, 1929.
44 J. Rieger, *Macromol. Rapid Commun.*, 2015, **36**, 1458.
45 A. Blanazs, A. J. Ryan and S. P. Armes, *Macromolecules*, 2012, **45**, 5099.
46 A. Blanazs, S. P. Armes and A. J. Ryan, *Macromol. Rapid Commun.*, 2009, **30**, 267.
47 J. N. Israelachvili, D. J. Mitchell and B. W. Ninham, *J. Chem. Soc., Faraday Trans. 2*, 1976, **72**, 1525.
48 C. J. Ferguson, R. J. Hughes, D. Nguyen, B. T. T. Pham, R. G. Gilbert, A. K. Serelis, C. H. Such and B. S. Hawkett, *Macromolecules*, 2005, **38**, 2191.
49 D. E. Ganeva, E. Sprong, H. De Bruyn, G. G. Warr, C. H. Such and B. S. Hawkett, *Macromolecules*, 2007, **40**, 6181.
50 N. P. Truong, M. V. Dussert, M. R. Whittaker, J. F. Quinn and T. P. Davis, *Polym. Chem.*, 2015, **6**, 3865.
51 I. Chaduc, A. Crepet, O. Boyron, B. Charleux, F. D'Agosto and M. Lansalot, *Macromolecules*, 2013, **46**, 6013.
52 S. Binauld, L. Delafresnaye, B. Charleux, F. D'Agosto and M. Lansalot, *Macromolecules*, 2014, **47**, 3461.
53 M. J. Derry, L. A. Fielding and S. P. Armes, *Prog. Polym. Sci.*, 2016, **52**, 1.
54 N. J. Warren and S. P. Armes, *J. Am. Chem. Soc.*, 2014, **136**, 10174.
55 S. L. Canning, G. N. Smith and S. P. Armes, *Macromolecules*, 2016, **49**, 1985.
56 J. V. M. Weaver, I. Bannister, K. L. Robinson, X. Bories-Azeau, S. P. Armes, M. Smallridge and P. McKenna, *Macromolecules*, 2004, **37**, 2395.
57 Y. Xia, N. A. D. Burke and H. D. H. Stöver, *Macromolecules*, 2006, **39**, 2275.
58 P. A. FitzGerald, S. Gupta, K. Wood, S. Perrier and G. G. Warr, *Langmuir*, 2014, **30**, 7986.
59 N. J. W. Penfold, J. R. Lovett, N. J. Warren, P. Verstraete, J. Smets and S. P. Armes, *Polym. Chem.*, 2016, **7**, 79.
60 J. R. Lovett, N. J. Warren, S. P. Armes, M. J. Smallridge and R. B. Cracknell, *Macromolecules*, 2016, **49**, 1016.
61 J. R. Lovett, N. J. Warren, L. P. D. Ratcliffe, M. K. Kocik and S. P. Armes, *Angew. Chem., Int. Ed.*, 2015, **54**, 1279.
62 J.-F. Baussard, J.-L. Habib-Jiwan, A. Laschewsky, M. Mertoglu and J. Storsberg, *Polymer*, 2004, **45**, 3615.
63 M. Mertoglu, A. Laschewsky, K. Skrabania and C. Wieland, *Macromolecules*, 2005, **38**, 3601.
64 A. B. Lowe and C. L. McCormick, *RAFT polymerization in homogeneous aqueous media: initiation systems,*

*RAFT agent stability, monomers and polymer structures*, Wiley-VCH Verlag GmbH & Co. KGaA, Weinheim, Germany, 2008.
65 S. Sugihara, A. Blanazs, S. P. Armes, A. J. Ryan and A. L. Lewis, *J. Am. Chem. Soc.*, 2011, **133**, 15707.
66 H. Ohshima, *Langmuir*, 2015, **31**, 13633.
67 A. Blanazs, R. Verber, O. O. Mykhaylyk, A. J. Ryan, J. Z. Heath, C. W. Douglas and S. P. Armes, *J. Am. Chem. Soc.*, 2012, **134**, 9741.
68 R. Verber, A. Blanazs and S. P. Armes, *Soft Matter*, 2012, **8**, 9915.
69 M. K. Kocik, O. O. Mykhaylyk and S. P. Armes, *Soft Matter*, 2014, **10**, 3984.
70 A. Rank, S. Hauschild, S. Förster and R. Schubert, *Langmuir*, 2009, **25**, 1337.
71 C. J. Mable, R. R. Gibson, S. Prevost, B. E. McKenzie, O. O. Mykhaylyk and S. P. Armes, *J. Am. Chem. Soc.*, 2015, **137**, 16098.